Exhaustive Mutagenesis of Six Secondary Active-Site Residues in *Escherichia coli* Chorismate Mutase Shows the Importance of Hydrophobic Side Chains and a Helix N-Capping Position for Stability and Catalysis†

Jonathan Kyle Lassila,‡ Jennifer R. Keeffe,‡ Peter Kast,§ and Stephen L. Mayo*,||

Division of Biology, Division of Chemistry and Chemical Engineering, and Howard Hughes Medical Institute, California Institute of Technology, Pasadena, California 91125, and Laboratory of Organic Chemistry, ETH Zurich, CH-8093 Zurich, Switzerland

Received January 31, 2007; Revised Manuscript Received April 12, 2007

ABSTRACT: Secondary active-site residues in enzymes, including hydrophobic amino acids, may contribute to catalysis through critical interactions that position the reacting molecule, organize hydrogen-bonding residues, and define the electrostatic environment of the active site. To ascertain the tolerance of an important model enzyme to mutation of active-site residues that do not directly hydrogen bond with the reacting molecule, all 19 possible amino acid substitutions were investigated in six positions of the engineered chorismate mutase domain of the *Escherichia coli* chorismate mutase−prephenate dehydratase. The six secondary active-site residues were selected to clarify results of a previous test of computational enzyme design procedures. Five of the positions encode hydrophobic side chains in the wild-type enzyme, and one forms a helix N-capping interaction as well as a salt bridge with a catalytically essential residue. Each mutant was evaluated for its ability to complement an auxotrophic chorismate mutase deletion strain. Kinetic parameters and thermal stabilities were measured for variants with *in vivo* activity. Altogether, we find that the enzyme tolerated 34% of the 114 possible substitutions, with a few mutations leading to increases in the catalytic efficiency of the enzyme. The results show the importance of secondary amino acid residues in determining enzymatic activity, and they point to strengths and weaknesses in current computational enzyme design procedures.

Chorismate mutases catalyze the Claisen rearrangement of chorismate to prephenate (Scheme 1). This reaction is an essential step in the biosynthesis of aromatic compounds including tyrosine and phenylalanine in plants, bacteria, and fungi. Isotope studies have established that both solution and enzyme-catalyzed rearrangements proceed through a chairlike transition state (*1*, *2*) in a concerted, asynchronous [3,3]-sigmatropic process (*3*−*5*).

As an intramolecular reaction that appears to be catalyzed without intermediate steps, covalent catalysis, or modification of the reaction pathway, the chorismate−prephenate rearrangement has become an important model system for theoretical approaches to the study of enzyme catalysis (recently reviewed in ref *6*). These same features make the reaction a compelling model for evaluating procedures for computational enzyme design. In earlier work (*7*), we tested

Scheme 1

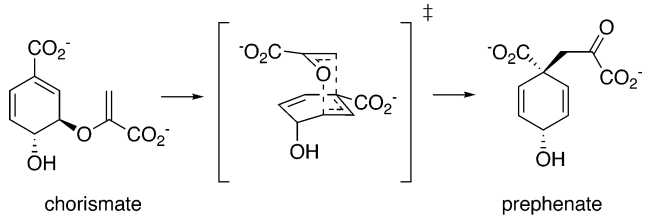

computational enzyme design methods (*8*) through redesign of the active site of a chorismate mutase. Amino acid identities and conformations were optimized for 18 active-site residues in the presence of an *ab initio* calculated transition state structure. The calculation returned wild-type residues in 12 of 18 designed positions, and the six mutations predicted by the calculation were to amino acids that do not make hydrogen bond contacts to the reacting molecule. Because the active-site environment is likely to present significant challenges to protein design energy functions that are typically tuned for global stability (*9*, *10*), we sought to better define the consequences for both stability and catalysis of mutating these six secondary active-site positions of the natural enzyme.

Two structurally distinct chorismate mutase forms have been identified. While the *Bacillus subtilis* enzyme (BsCM)[1] and other AroH mutases adopt a homotrimeric pseudo-α/*β*-barrel fold (*11*), the AroQ mutases from *Escherichia coli*

† This work was supported by the Howard Hughes Medical Institute, the Defense Advanced Research Projects Agency, the Institute for Collaborative Biotechnologies (ARO), the Ralph M. Parsons foundation, and an IBM Shared University Research Grant.

* To whom correspondence should be addressed. Mailing address: California Institute of Technology, 1200 E. California Blvd, MC 114-96, Pasadena, CA 91125. E-mail: steve@mayo.caltech.edu. Phone: (626) 395-6408. Fax: (626) 568-0934.

‡ Biochemistry Option, California Institute of Technology.

§ Laboratory of Organic Chemistry, ETH Zurich.

|| Division of Biology, Division of Chemistry and Chemical Engineering, and the Howard Hughes Medical Institute, California Institute of Technology.

10.1021/bi700215x CCC: $37.00
Published on Web 05/17/2007

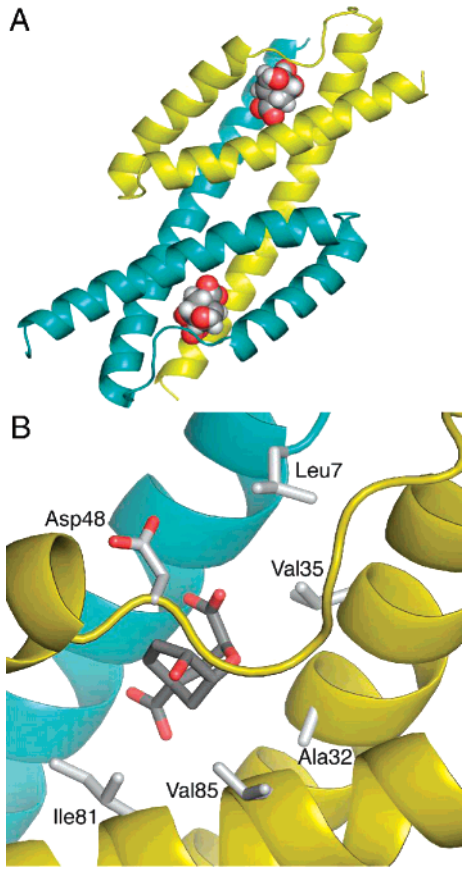

FIGURE 1: Truncated, monofunctional chorismate mutase domain from *E. coli* chorismate mutase−prephenate dehydratase in complex with a transition state analog (dark gray carbons), from pdb code 1ecm: (A) overall fold, showing the two chains of the symmetric homodimer in teal and gold with the bound transition state analog shown as a CPK model; (B) active-site residues investigated in this study shown with light gray carbon atoms.

and other organisms are all-helical proteins (*12*−*15*). Chorismate mutases from *E. coli* are fused to their downstream biosynthetic partners, yielding bifunctional chorismate mutase−prephenate dehydratase (P-protein) and chorismate mutase−prephenate dehydrogenase (T-protein) enzymes (*16*). Mechanistic investigations of the bifunctional T-protein enzyme were complicated by a rate-limiting step other than the Claisen rearrangement (*3*). However, truncated, monofunctional constructs of the P-protein (Figure 1A, referred to as EcCM herein) have permitted structural and mechanistic studies of an isolated AroQ chorismate domain (*17*). The rearrangement catalyzed by EcCM shows expected patterns of kinetic isotope effects and no sensitivity to viscosogens, strongly suggesting that the Claisen rearrangement is the rate-determining step (*5*, *18*). In contrast, BsCM appears to be limited partially by a diffusive process and partially by the chemical step (*4*, *18*).

Previous mutagenesis and selection studies of both EcCM and BsCM enzymes have demonstrated that efficient catalysis depends on positively charged active-site residues poised to interact with substrate carboxylates and ether oxygen as well as negatively charged side chains able to contact the substrate hydroxyl group (*19*−*25*).

[1] Abbreviations: EcCM, chorismate mutase domain of *E. coli* chorismate mutase−prephenate dehydratase (P-protein); BsCM, *Bacillus subtilis* chorismate mutase; CD, circular dichroism.

The present work focuses on secondary active-site side chains that do not hydrogen bond with the reacting molecule but nonetheless may participate in catalysis by positioning the substrate, organizing charged and polar active-site residues, or defining the electrostatic environment of the active site (*26*−*31*). The impact of secondary active-site residues on catalytic activity is an important concern for *de novo* computational enzyme design efforts, because common methods strongly emphasize placement of primary catalytic residues (*8*, *32*−*35*). Secondary active-site residues may also have special consequences for enzyme stability. Prior mutagenesis studies have found inverse relationships between changes in protein stability and changes in activity following the mutation of active-site residues, consistent with a notion that creation of a cavity with specialized electrostatic properties opposes the normal driving forces of protein stability (*36*−*40*).

We have evaluated the effects of all 19 possible single mutations to the six EcCM active-site residues that were mutated in our previous computational design experiment: Leu7, Ala32, Val35, Asp48, Ile81, and Val85 (Figure 1B). Each of the 114 variants was tested for complementation of the chorismate mutase deficiency of the auxotrophic *E. coli* KA12/pKIMP-UAUC system of Kast, Hilvert, and coworkers (*22*). Biologically active variants were purified, and their *in vitro* thermal stabilities and steady-state kinetic parameters were assessed.

MATERIALS AND METHODS

Materials and Strains. *E. coli* KA12 and plasmid pKIMP-UAUC have been described previously (*22*, *41*). Chorismic acid (97.5%) was purchased from Sigma-Aldrich.

Construction and in Vivo Evaluation of Mutants. The chorismate mutase domain (consisting of the 109 N-terminal residues of the P-protein) described by Ganem and coworkers (*17*) was previously fused to the C-terminus of a self-cleavable chitin binding domain−intein fusion construct (IMPACT-CN, New England Biolabs) (*7*). The QuikChange multisite mutagenesis kit (Stratagene) was used to create site-specific variants in this construct by using single oligonucleotides bearing degenerate codons (i.e., NNK) in the position of interest. After transformation of XL10-gold cells (Stratagene), DNA was prepared directly from plated colonies and subsequently used to transform KA12/pKIMP-UAUC. Cells were plated on both selective media and nonselective media. M9c minimal agar plates were prepared as described (*42*) except that 20 μg/mL L-phenylalanine was included in the selective plates (nonselective plates contained both L-phenylalanine and L-tyrosine). To facilitate identification of active variants, mutagenesis reactions were performed with inactive templates (i.e., stop codons in the position of interest), and DNA was sequenced from viable colonies on selective media. Inactive variants were identified by performing the mutagenesis reaction on a wild-type template and looking for colonies that were nonviable when streaked onto selective media plates. To recover missing variants, mutagenesis reactions with nondegenerate and less-degenerate oligonucleotides were performed. Biological activity or inactivity was confirmed by retransformation of isolated plasmid DNA and plating on selective and nonselective media. All reported constructs were verified by DNA sequencing over the entire EcCM coding region.

Because the N-terminal gene fusion was not sequenced for each variant, we investigated the possibility that disruption of activity might be caused by deleterious mutations to the promoter region or the N-terminally fused chitin-binding/intein region rather than by mutation of the enzyme itself. Evidence against such artifacts was provided for some inactive variants by multiple independent occurrences of the same mutation with identical behavior. For the remaining inactive variants, small-scale expression tests followed by SDS−PAGE verified the presence of appropriately sized, overproduced protein. Any frameshift within the N-terminal fusion protein would encounter multiple stop codons leading to a visibly truncated protein. Similar expression tests of the N-terminal fusion protein alone showed that the size difference was readily apparent.

In position 48, some variants displayed ambiguous behavior, with only a few colonies growing on selective media. For position 48 variants, an arbitrary threshold was applied, such that a variant was considered biologically active if at least 10% of the number of colonies were observed on selective media as on nonselective media when equal amounts were plated. This resulted in a stringent test for activity, where active variants exhibited at least 5% of wild-type k_{cat}/K_m.

Protein Overproduction and Purification. Biologically active constructs were expressed in *E. coli* BL21 DE3. Overexpression was induced with 1 mM IPTG followed by growth at room temperature. Cells were lysed using an Emulsiflex-C5 (Avestin), and the fusion proteins were affinity purified with chitin agarose (New England Biolabs). Affinity tag self-cleavage was induced with 50 mM DTT at 25 °C. Mass spectrometry and SDS−PAGE previously indicated that this procedure results in the desired EcCM construct (*7*). Proteins were further purified by gel filtration in 50 mM Tris-HCl, pH 7.8, 100 mM NaCl. A well-resolved dimer peak was collected, and variants with significant higher-order aggregation were not further considered. We expected that affinity purification followed by gel filtration would eliminate any significant catalytic contribution of endogenous *E. coli* CM enzymes, since they do not have the affinity tag and are considerably larger in size. In fact, no activity was detected when concentrated extracts from cells harboring empty pTYB-11 fusion vector were subjected to identical purification steps and assay procedures. For consistency with previously published kinetic studies of the same construct (*7*, *23*, *43*), protein concentration was determined by the Bradford assay using BSA as a standard (Bio-Rad).

CD Spectrometry and Thermal Denaturation. Far-UV circular dichroism (CD) spectra were collected at the activity assay temperature of 37 °C. All variants showed nearly superimposable wavelength scans. Thermostability was assessed by thermal denaturation monitored by CD at 222 nm. CD was monitored using an Aviv 62DS spectrometer and a 1 mm path length cell. Increments of 1 °C were used with an equilibration time of 90 s and a signal averaging time of 30 s. Buffer conditions were 50 mM Tris-HCl, pH 7.8, 100 mM NaCl. Midpoints of thermal denaturation (T_m) were obtained by fitting the data to a two-state model (*44*). It should be noted, however, that unfolding was not reversible and some samples showed clear evidence of non-two-state behavior, so T_m values should be taken as estimates of relative stabilities rather than thermodynamic parameters. CD data were collected at 22 ± 3 μM protein. Variations in T_m from different concentrations within the range were similar to variations across multiple trials.

Kinetic Assays. Activities were measured by following the absorbance of chorismate at 275 nm ($\epsilon = 2630$ M^{-1} cm^{-1} (*3*)). Activity assays were performed at 37 °C in 50 mM Tris-HCl, pH 7.8, 2.5 mM EDTA, 20 mM β-mercaptoethanol, and 0.01% BSA, conditions used in prior studies of the same construct (*7*, *23*, *43*). Given pK_a's for chorismate and prephenate of <4.5 (*45*), these conditions ensure that the reaction of chorismate^{2-} to prephenate^{2-} was monitored. A protein concentration of 20 nM was generally used; however, less-active variants were assayed with 40 or 100 nM protein. For cases where k_{cat} and K_m are reported, at least three trials with nine or more data points each were performed, and substrate concentration ranges of at least 0.3−3 times K_m were used. Kinetic parameters were determined by nonlinear fitting of the buffer-corrected initial rates to the Michaelis−Menten equation.

RESULTS

The effects of all possible single amino acid substitutions were evaluated in six positions in the chorismate mutase domain of the *E. coli* P-protein (Table 1). Each construct was evaluated for its ability to complement the KA12/pKIMP-UAUC system (*22*, *41*), which requires chorismate mutase activity for viability in media lacking tyrosine and phenylalanine. Of the 114 mutants, 39 (or 34%) were scored as active.

EcCM variants promoting viability were purified, and their *in vitro* stabilities and kinetic parameters were evaluated. Of the mutants active *in vivo*, measured T_m values ranged approximately ±10 °C relative to wild type, yet the average T_m (61.6 °C) was remarkably similar to that of the wild type (61.4 °C). *In vitro* enzyme activities were reduced relative to wild type, except in a few cases. The greatest increase in activity relative to wild type was found with the Ala32Ser mutation, previously reported as the result of a computational design approach (*7*). This mutation results in an approximately 60% increase in catalytic efficiency with less than 1 °C change in T_m.

Position 7. Based on the wild-type structure with bound transition state analog (1ecm), Leu7 lies near the carboxylate of the enolpyruvyl moiety, and the catalytically essential residue Arg11 is sandwiched between Leu7 and Arg51 from the adjacent helix. Six relatively conservative side chain substitutions were tolerated in this position. Substitution of phenylalanine or isoleucine for wild-type leucine maintained catalytic efficiency within 10%, and the leucine to isoleucine mutation increased T_m by 4.4 °C.

Position 32. Ala32 lies closest to the forming C−C bond and the cyclohexadienyl face carboxylate, based on the 1ecm structure. Although six alternative side chains were tolerated in position 32, only the Ala32Ser and Ala32Thr variants could be readily purified without precipitation or aggregation. The Ala32Ser and Ala32Thr mutations increased catalytic efficiency by 62% and 23%, respectively.

Position 35. Val35 is expected to pack against the enolpyruvyl moiety of the reacting molecule. In addition, this residue closely neighbors the catalytically important

Table 1: Results for Complementation Tests, Kinetic Parameters, and Thermal Stabilities[a]

pos 7	C/NC[b]	k_{cat}, s^{-1}	K_m, μM	k_{cat}/K_m, M^{-1} s^{-1}	T_m, °C	pos 48	C/NC[b]	k_{cat}, s^{-1}	K_m, μM	k_{cat}/K_m, M^{-1} s^{-1}	T_m, °C
Ala	−					Ala	−				
Arg	−					Arg	−				
Asn	−					Asn	+		>750	7.9×10^3	56.5
Asp	−					Asp*	+	**39 ± 5**	**300 ± 50**	**1.3×10^5**	**61.4 ± 0.6**
Cys	+		>750	1.0×10^4	52.0	Cys	+		>750	1.8×10^4	53.8
Gln	−					Gln	+		>750	9.8×10^3	55.5
Glu	−					Glu	−				
Gly	−					Gly	−				
His	−					His	−				
Ile	+	36 ± 2	300 ± 80	1.2×10^5	65.8	Ile	−				
Leu*	+	**39 ± 5**	**300 ± 50**	**1.3×10^5**	**61.4 ± 0.6**	Leu	+		>750	7.1×10^3	57.7
Lys	−					Lys	−				
Met	+		>750	4.4×10^4	60.3	Met	−				
Phe	+	48 ± 2	350 ± 30	1.4×10^5	62.3	Phe	−				
Pro	−					Pro	−				
Ser	−					Ser	−				
Thr	+		>750	1.3×10^4	59.2	Thr	−				
Trp	−					Trp	−				
Tyr	−					Tyr	−				
Val	+	36 ± 3	700 ± 100	5×10^4	61.9	Val	−				

pos 32	C/NC[b]	k_{cat}, s^{-1}	K_m, μM	k_{cat}/K_m, M^{-1} s^{-1}	T_m, °C	pos 81	C/NC[b]	k_{cat}, s^{-1}	K_m, μM	k_{cat}/K_m, M^{-1} s^{-1}	T_m, °C
Ala*	+	**39 ± 5**	**300 ± 50**	**1.3×10^5**	**61.4 ± 0.6**	Ala	−				
Arg	−					Arg	−				
Asn	−					Asn	−				
Asp	−					Asp	−				
Cys	+				aggr	Cys	+				aggr
Gln	−					Gln	−				
Glu	−					Glu	−				
Gly	+				aggr	Gly	−				
His	−					His	−				
Ile	+				aggr	Ile*	+	**39 ± 5**	**300 ± 50**	**1.3×10^5**	**61.4 ± 0.6**
Leu	−					Leu	+		>750	5.5×10^4	57.7
Lys	−					Lys	−				
Met	−					Met	+	27 ± 2	270 ± 20	1.0×10^5	64.6
Phe	−					Phe	+		>750	8.7×10^3	59.0
Pro	−					Pro	−				
Ser	+	45 ± 6	220 ± 30	2.1×10^5	61.7	Ser	−				
Thr	+	61 ± 4	380 ± 70	1.6×10^5	62.8	Thr	−				
Trp	−					Trp	+				aggr
Tyr	−					Tyr	−				
Val	+				aggr	Val	+				aggr

pos 35	C/NC[b]	k_{cat}, s^{-1}	K_m, μM	k_{cat}/K_m, M^{-1} s^{-1}	T_m, °C	pos 85	C/NC[b]	k_{cat}, s^{-1}	K_m, μM	k_{cat}/K_m, M^{-1} s^{-1}	T_m, °C
Ala	+	20 ± 2	520 ± 90	3.9×10^4	61.2	Ala	+		>750	1.2×10^4	62.7
Arg	−					Arg	+		>750	4.2×10^4	66.9
Asn	−					Asn	+		>750	1.2×10^4	66.8
Asp	−					Asp	−				
Cys	+	18.6 ± 0.6	360 ± 40	5.2×10^4	61.8	Cys	+	32 ± 4	570 ± 90	5.4×10^4	54.7
Gln	−					Gln	−				
Glu	−					Glu	−				
Gly	−					Gly	−				
His	−					His	−				
Ile	+	65 ± 9	440 ± 80	1.5×10^5	66.6	Ile	+	55 ± 1	550 ± 30	1.0×10^5	62.9
Leu	+		>750	1.3×10^4	66.7	Leu	+		>750	4.3×10^4	62.2
Lys	−					Lys	+		>750	1.3×10^4	67.1
Met	+		>750	5.2×10^4	68.9	Met	+		>750	1.5×10^4	65.6
Phe	−					Phe	+		>750	2.1×10^4	61.7
Pro	−					Pro	−				
Ser	−					Ser	−				
Thr	+		>750	2.0×10^4	56.5	Thr	+		>750	2.2×10^4	62.1
Trp	−					Trp	+				aggr
Tyr	−					Tyr	+		>750	2.6×10^4	65.7
Val*	+	**39 ± 5**	**300 ± 50**	**1.3×10^5**	**61.4 ± 0.6**	Val*	+	**39 ± 5**	**300 ± 50**	**1.3×10^5**	**61.4 ± 0.6**

[a] Assays were performed at 37 °C and pH 7.8; see Materials and Methods. Wild-type residues are indicated with bold type and asterisks, and wild-type values differ by less than 5% from published values for the same construct and conditions (*23, 43*). aggr indicates that protein precipitated or aggregated during purification. Where uncertainties are indicated, the means and standard deviations from at least three trials are reported. [b] Variants complementing the deletion strain are indicated by +, noncomplementing by −.

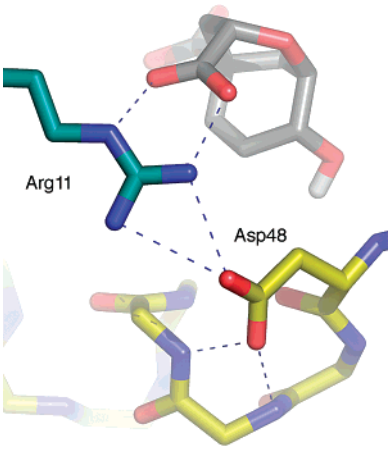

FIGURE 2: Interactions of Asp48 with the N-terminus of the second helix and with Arg11. The carbon atoms of the bound transition state analog are in gray, while those of the side chains are colored in teal and gold to indicate their association with the corresponding EcCM chain. Many side chains, protons, and other elements are omitted for clarity.

residues Lys39 and Gln88, both of which contact the ether oxygen of the breaking bond. Six substitutions were tolerated in this position, with four leading to increased thermostability. The Val35Met, Val35Leu, and Val35Ile mutations increased T_m by 7.5, 5.3, and 5.2 °C, respectively. All mutations led to increased K_m, and all led to between 2- and 10-fold decreases in catalytic efficiency except for Val35Ile, which showed a 15% increase.

Position 48. In the wild-type structure, Asp48 hydrogen bonds with both the N-terminus of the second helix in EcCM and Arg11, a critical residue that contacts the transition state analog in the crystal structure (Figure 2). Four position 48 mutants were scored as biologically active, and all four showed reductions in T_m of 3−8 °C and large increases in K_m.

Position 81. Ile81 is expected to pack closely against the cyclohexadienyl face carboxylate of the reacting molecule. Six substitutions of this residue were tolerated, although the cysteine, tryptophan, and valine mutants were prone to aggregation *in vitro*. Aside from a 3.2 °C increase in stability with the Ile81Met mutation, the substitutions for which data could be obtained led to reduced stability and catalytic efficiency.

Position 85. Val85 lies adjacent to Ile81 and close to the cyclohexadienyl face of the reacting molecule at the breaking bond carbon, based on the 1ecm structure. Its Cα−Cβ vector is directed more toward solvent than that of Ile81, however. Position 85 was broadly tolerant of substitution, allowing 12 of 19 possible mutations. Interestingly, 9 of the 11 mutants for which data were recorded resulted in increased T_m relative to wild-type, while all of the mutants yielded significant increases in K_m.

DISCUSSION

Tolerance to Mutation. In this study, 34% of all single mutants were scored as biologically active. While it is difficult to compare results across systems because of variations in cellular requirements, expression levels, initial protein stability (*46*−*48*), and various other factors, this value is consistent with other mutational studies. A sampling from among the many exhaustive and random mutagenesis studies suggests that between 50% and 85% of single mutations typically maintain some level of function, while in catalytic sites, 20−60% on average preserve some function (*49*−*57*). Thus, the amino acid positions studied here have tolerances to single mutation that are similar to active-site residues in other enzymes.

Helix N-Capping Position. The N-termini of α helices are preceded by residues with distinct preferences for side chains that can satisfy unpaired helical hydrogen bond donors. These N-capping residues are reflected in protein database surveys, protein stability measurements, and model peptide studies (reviewed in ref *58*). N-cap residues can affect helix stability by as much as 4 kcal/mol (*59*) and are found to be important considerations in protein design (*60*). The 1ecm crystal structure suggests that Asp48 occupies an ideal geometry for simultaneous N-capping and salt bridge formation with Arg11, a critical residue that contacts the transition state analog (Figure 2). Mutational studies have shown the importance of Arg11 to catalysis; the Arg11Lys and Arg11Ala mutations lead to 10^3-fold and 10^4-fold reduction in catalytic efficiency, respectively (*20*).

The reduction in stability of all biologically active position 48 variants coincides with previous studies placing aspartic acid as one of the most favored N-capping residues (*61*−*63*). The loss in activity upon mutation may suggest that the Asp48−Arg11 salt bridge is important for positioning of the catalytically important arginine. Alternatively, the interaction may have a role in the substrate binding process. The salt bridge spans the interface between two helices proposed to offer the site of entry into the binding pocket. Structural studies on related enzymes suggest that these two helices move relative to each other, potentially opening an entry pathway (*14*). Mutations in position 48 could conceivably interfere with the substrate entry process, which may be reflected in the increased K_m values. The fact that Asp48Asn and Asp48Gln mutants were scored as active while Asp48Glu was not could suggest that a very precise geometric positioning is required for the catalytic process, which may be compromised in a backbone−Glu48−Arg11 hydrogen bond network.

Comparison to Other AroQ Family Members. Table 2 shows the structural equivalents of each of the six residues in crystal structures of AroQ chorismate mutases from four other organisms. For each structure, sequence variations among closely related homologs were determined by BLAST searches of the RefSeq database (*64*, *65*). A number of the sequence variations seen in the homologs were found to retain wild-type-like or have increased activity in the EcCM scaffold: Leu7Ile, Ala32Ser, Ala32Thr, and Val35Ile. Four other mutations were also observed in the sequence alignments but led to precipitated or aggregated protein *in vitro*: Ala32Val, Ala32Gly, Ala32Cys, and Ile81Val. The majority of the alternative residues found in the sequence alignments, however, led in EcCM to reduced *in vitro* activity or loss of function in the *in vivo* assay. Clearly, sequence alignments provide information about possible substitution tolerances in a given enzyme scaffold, but activity is ultimately determined within the structural context of the specific protein.

The considerable tolerance to mutation seen with position 85 is also reflected in the sequence alignments. Related

Table 2: Structural Alignment of Solved AroQ Mutase Structures and BLAST Results[a]

E. coli; 1ecm	Leu7	Ala32 [STV]	Val35 [I]	Asp48 [AEKQSTV]	Ile81 [L]	Val85
S. cerevisiae; 4csm	Leu12	Gly161	Val164	Asn194 [DYFKS]	Ile239 [M]	Lys243
M. tuberculosis; 2fp2	Leu130	Ala53	Val56 [IM]	Asp69	Ile102	Glu106 [KV]
P. furiosus; 1ybz	Leu4	Ala29 [CS]	Ile32 [M]	Asp45 [V]	Leu67 [V]	Lys71 [R]
T. thermophilus; 2d8d	Ile5 [LM]	Val30 [A]	Ile33 [V]	Asp46	Phe78	Leu82 [T]

[a] Structures from the pdb codes indicated were aligned over the transition state analog if present and otherwise over all residues. For each pdb protein sequence, protein−protein BLAST (*64*) was performed using the RefSeq database (*65*). Variations of the position are reported in brackets for matches with bitscores of 85 or greater (60 for 1ybz); these scores corresponded to sequences with ∼40% sequence identity or greater.

proteins feature alternatives including glutamic acid, lysine, and arginine, consistent with the higher solvent exposure of this position. While a previous selection study reported the equivalent of position 85 in *Methanococcus jannaschii* CM to be highly conserved (*66*), that observation may reflect interactions not present in the EcCM structure. The equivalent position is occupied by lysine in the *M. jannaschii* enzyme, as well as in the *Saccharomyces cerevisiae* and *Pyrococcus furiosus* enzymes, where crystal structures show the lysine engaging in salt bridge interactions with a neighboring helix (*13*). Curiously, the equivalent of position 85 in the *Mycobacterium tuberculosis* enzyme makes a catalytically important contact to the hydroxyl group of the transition state analog that replaces the interaction made in EcCM by Glu52 (*14*), again suggesting that the role of this position may be strongly scaffold-dependent.

In position 48, the sequence alignments showed much more variation in amino acid identity than was experimentally found to be compatible with EcCM function. Changes in helix register in some of the homologs may be partially responsible for these large variations.

Tradeoff between Stability and Activity. Various authors have considered the view that evolutionary optimization of active-site residues for binding of transition states would lead to selection of residues that are not optimal for protein stability (*36*−*40*). Implicit in the argument is the idea that stabilizing interactions that the enzyme devotes to the reacting molecule are both unsatisfied and likely destabilizing to the protein when the molecule is not bound. A laboratory-evolved chorismate mutase dramatically illustrated this principle by transforming from an apparent molten globule into a more ordered protein in the presence of a transition state analog (*67*, *68*).

Although a correlation was not seen between changes in stability and activity of the chorismate mutase variants studied here (see Supporting Information), some of the mutants are consistent with the notion of a stability−activity tradeoff. More mutants (20) showed increased stability than decreased stability (12). In position 85 of EcCM, all of the 11 biologically active mutants for which data could be obtained showed reduced catalytic efficiency and an increased K_m value and nearly all mutants exhibited increased thermostability. Because Val85 participates in van der Waals interactions with both the transition state analog and residues from neighboring helices in the 1ecm structure, chorismate binding and stability could be affected by altering the shape of the binding pocket or by interfering with helix−helix interactions that contribute to the structural fortitude of the active site. Specifically, movement of the neighboring helix has been proposed to facilitate substrate entry (*14*) and modified helix−helix interaction could thus affect substrate affinity. Also, in position 35, all biologically active mutations increased the K_m. While not all of the mutations led to increased T_m values, three showed increases in thermostability of more than 4 °C. Val35 in the 1ecm structure appears to participate in van der Waals interactions with the transition state analog, the catalytically important residues Lys39 and Gln88, and some neighboring helix residues. While the present study cannot be expected to determine the relative contributions of these interactions to EcCM function, it clearly suggests that this residue contributes to the catalytic process and the global stability of the protein.

Relationship to Models of EcCM Catalytic Mechanism. Among theorists, differing computational treatments of chorismate mutase systems have led to varied descriptions of the origin of enzymatic catalysis of the reaction. Despite an observation that the chemical step is not fully rate-limiting in the BsCM enzyme (*18*), the majority of work has modeled that active site (*69*−*87*). The few computational investigations of EcCM have proposed, in opposition to most of the other studies, that both enzymes accelerate the rearrangement exclusively by restricting the conformational space of the substrate and not by stabilizing the transition state (*78*, *88*−*90*). These studies, and an earlier one (*91*), explicitly identified Val35 and Ile81 as mediators of substrate conformational restriction. Although we find that both positions tolerate a number of mutations, we do not expect the data provided here to allow for differentiation between possible modes of EcCM catalysis.

For example, the Val35Ile mutation leads to an increase in k_{cat} and the Val35Ala mutation leads to a decreased k_{cat} value. While these mutations would be expected to reduce and increase the conformational freedom of the bound substrate, respectively, the changes in k_{cat} are relatively modest and could be attributed to any number of factors. In addition to its close proximity to the reacting molecule, Val35 is within van der Waals contact distance of the catalytically essential Lys39 and a number of other residues. Perturbations to any of these interactions could have consequences for the geometry and energetics of critical hydrogen bonds, leading to changes in relative stabilization of the transition state. Simple continuum electrostatics calculations suggest that these mutations could also lead to small changes in electrostatic potential at the reacting molecule. In short, hydrophobic active-site residues perform important functions in active sites, but it is difficult to isolate their precise effects on catalysis.

Implications for Enzyme Design. In the computational design experiment previously performed by our group (*7*), the global minimum energy sequence for 18 designed EcCM active-site residues contained mutations to only the six positions of the present study: Leu7Ile, Ala32Ser, Val35Ile, Asp48Ile, Ile81Leu, and Val85Ile. Of these six mutations, two were found to be the most active of all possible single

substitutions for the given amino acid position, and one was found to be the most stable variant of the amino acid position.

While the five hydrophobic positions were generally modeled well, the strong preference for aspartate in position 48 is not well represented by the molecular mechanics and rotamer library-based protein design approach. In typical energy models used for design, repulsion of the charged aspartate side chain with the carboxylate of the reacting molecule results in disfavoring of the wild-type position 48 residue. Regardless of whether Asp48 contributes to catalysis by positioning of the critical Arg11, solidifying the local structure around the helix N-terminus, or contributing to substrate entry into the binding site, the effect of this residue is likely due to complex and cooperative effects of Asp48 that are difficult to model in a design calculation. Present computational protein design models typically neglect explicit treatment of side-chain entropy, electron polarization, the unbound state of the protein, and changes in backbone structure, any of which could prove critical in defining the energetics that underlie the strong requirement for aspartate in position 48. The present dataset will enable a more detailed evaluation of the strengths and weaknesses of various energy functions for design.

Finally, the ability of EcCM to tolerate a number of mutations without reduction in stability or activity is in accord with previous descriptions of active-site plasticity. Secondary active-site positions that accept side chain substitutions can allow evolution or design of enzymes with new substrate specificities and chemical mechanisms, sometimes without disruption of the original function (*92*−*95*). These secondary positions offer rich opportunities for testing and refining enzyme design methodologies through active-site redesign experiments.

SUPPORTING INFORMATION AVAILABLE

A plot showing changes in activity with changes in stability for the mutants. This material is available free of charge via the Internet at http://pubs.acs.org.

REFERENCES

1. Sogo, S. G., Widlanski, T. S., Hoare, J. H., Grimshaw, C. E., Berchtold, G. A., and Knowles, J. R. (1984) Stereochemistry of the rearrangement of chorismate to prephenate: Chorismate mutase involves a chair transition state, *J. Am. Chem. Soc. 106*, 2701−2703.
2. Copley, S. D., and Knowles, J. R. (1985) The uncatalyzed Claisen rearrangement of chorismate to prephenate prefers a transition state of chairlike geometry, *J. Am. Chem. Soc. 107*, 5306−5308.
3. Addadi, L., Jaffe, E. K., and Knowles, J. R. (1983) Secondary tritium isotope effects as probes of the enzymic and nonenzymic conversion of chorismate to prephenate, *Biochemistry 22*, 4494−4501.
4. Gustin, D. J., Mattei, P., Kast, P., Wiest, O., Lee, L., Cleland, W. W., and Hilvert, D. (1999) Heavy atom isotope effects reveal a highly polarized transition state for chorismate mutase, *J. Am. Chem. Soc. 121*, 1756−1757.
5. Wright, S. K., DeClue, M. S., Mandal, A., Lee, L., Wiest, O., Cleland, W. W., and Hilvert, D. (2005) Isotope effects on the enzymatic and nonenzymatic reactions of chorismate, *J. Am. Chem. Soc. 127*, 12957−12964.
6. Gao, J. L., Ma, S. H., Major, D. T., Nam, K., Pu, J. Z., and Truhlar, D. G. (2006) Mechanisms and free energies of enzymatic reactions, *Chem. Rev. 106*, 3188−3209.
7. Lassila, J. K., Keeffe, J. R., Oelschlaeger, P., and Mayo, S. L. (2005) Computationally designed variants of *Escherichia coli* chorismate mutase show altered catalytic activity, *Protein Eng. Des. Sel. 18*, 161−163.
8. Lassila, J. K., Privett, H. K., Allen, B. D., and Mayo, S. L. (2006) Combinatorial methods for small-molecule placement in computational enzyme design, *Proc. Natl. Acad. Sci. U.S.A. 103*, 16710−16715.
9. Mendes, J., Guerois, R., and Serrano, L. (2002) Energy estimation in protein design, *Curr. Opin. Struct. Biol. 12*, 441−446.
10. Vizcarra, C. L., and Mayo, S. L. (2005) Electrostatics in computational protein design, *Curr. Opin. Chem. Biol. 9*, 622−626.
11. Chook, Y. M., Ke, H. M., and Lipscomb, W. N. (1993) Crystal structures of the monofunctional chorismate mutase from *Bacillus subtilis* and its complex with a transition state analog, *Proc. Natl. Acad. Sci. U.S.A. 90*, 8600−8603.
12. Lee, A. Y., Karplus, P. A., Ganem, B., and Clardy, J. (1995) Atomic structure of the buried catalytic pocket of *Escherichia coli* chorismate mutase, *J. Am. Chem. Soc. 117*, 3627−3628.
13. Xue, Y. F., Lipscomb, W. N., Graf, R., Schnappauf, G., and Braus, G. (1994) The crystal structure of allosteric chorismate mutase at 2.2-Ångstrom resolution, *Proc. Natl. Acad. Sci. U.S.A. 91*, 10814−10818.
14. Ökvist, M., Dey, R., Sasso, S., Grahn, E., Kast, P, and Krengel, U. (2006) 1.6 Å crystal structure of the secreted chorismate mutase from *Mycobacterium tuberculosis*: Novel fold topology revealed, *J. Mol. Biol. 357*, 1483−1499.
15. Kim, S.-K., Reddy, S. K., Nelson, B. C., Vasquez, G. B., Davis, A., Howard, A. J., Patterson, S., Gilliland, G. L., Ladner, J. E., and Reddy, P. T. (2006) Biochemical and structural characterization of the secreted chorismate mutase (Rv1885c) from *Mycobacterium tuberculosis* $H_{37}R_v$: an *AroQ enzyme not regulated by the aromatic amino acids, *J. Bacteriol. 188*, 8638−8648.
16. Cotton, R. G. H., and Gibson, F. (1965) The biosynthesis of phenylalanine and tyrosine: Enzymes converting chorismic acid into prephenic acid and their relationships to prephenate dehydratase and prephenate dehydrogenase, *Biochim. Biophys. Acta 100*, 76−88.
17. Stewart, J., Wilson, D. B., and Ganem, B. (1990) A genetically engineered monofunctional chorismate mutase, *J. Am. Chem. Soc. 112*, 4582−4584.
18. Mattei, P., Kast, P., and Hilvert, D. (1999) *Bacillus subtilis* chorismate mutase is partially diffusion-controlled, *Eur. J. Biochem. 261*, 25−32.
19. Cload, S. T., Liu, D. R., Pastor, R. M., and Schultz, P. G. (1996) Mutagenesis study of active-site residues in chorismate mutase from *Bacillus subtilis*, *J. Am. Chem. Soc. 118*, 1787−1788.
20. Liu, D. R., Cload, S. T., Pastor, R. M., and Schultz, P. G. (1996) Analysis of active-site residues in *Escherichia coli* chorismate mutase by site-directed mutagenesis, *J. Am. Chem. Soc. 118*, 1789−1790.
21. Kast, P., Hartgerink, J. D., Asif-Ullah, M., and Hilvert, D. (1996) Electrostatic catalysis of the Claisen rearrangement: Probing the role of Glu78 in *Bacillus subtilis* chorismate mutase by genetic selection, *J. Am. Chem. Soc. 118*, 3069−3070.
22. Kast, P., Asif-Ullah, M., Jiang, N., and Hilvert, D. (1996) Exploring the active site of chorismate mutase by combinatorial mutagenesis and selection: The importance of electrostatic catalysis, *Proc. Natl. Acad. Sci. U.S.A. 93*, 5043−5048.
23. Zhang, S., Kongsaeree, P., Clardy, J., Wilson, D. B., and Ganem, B. (1996) Site-directed mutagenesis of monofunctional chorismate mutase engineered from the *E. coli* P-protein, *Bioorg. Med. Chem. 4*, 1015−1020.
24. Kast, P., Grisostomi, C., Chen, I. A., Li, S. L., Krengel, U., Xue, Y. F., and Hilvert, D. (2000) A strategically positioned cation is crucial for efficient catalysis by chorismate mutase, *J. Biol. Chem. 275*, 36832−36838.
25. Kienhöfer, A., Kast, P., and Hilvert, D. (2003) Selective stabilization of the chorismate mutase transition state by a positively charged hydrogen bond donor, *J. Am. Chem. Soc. 125*, 3206−3207.
26. Warshel, A. (1978) Energetics of enzyme catalysis, *Proc. Natl. Acad. Sci. U.S.A. 75*, 5250−5254.
27. Honig, B., and Nicholls, A. (1995) Classical electrostatics in biology and chemistry, *Science 268*, 1144−1149.
28. Warshel, A. (1998) Electrostatic origin of the catalytic power of enzymes and the role of preorganized active sites, *J. Biol. Chem. 273*, 27035−27038.
29. Shan, S. O., and Herschlag, D. (1996) The change in hydrogen bond strength accompanying charge rearrangement: Implications for enzymatic catalysis, *Proc. Natl. Acad. Sci. U.S.A. 93*, 14474−14479.

30. Kraut, D. A., Carroll, K. S., and Herschlag, D. (2003) Challenges in enzyme mechanism and energetics, *Annu. Rev. Biochem. 72*, 517−571.
31. Benkovic, S. J., and Hammes-Schiffer, S. (2003) A perspective on enzyme catalysis, *Science 301*, 1196−1202.
32. Hellinga, H. W., and Richards, F. M. (1991) Construction of new ligand binding sites in proteins of known structure, *J. Mol. Biol. 222*, 763−785.
33. Bolon, D. N., and Mayo, S. L. (2001) Enzyme-like proteins by computational design, *Proc. Natl. Acad. Sci. U.S.A. 98*, 14274−14279.
34. Dwyer, M. A., Looger, L. L., and Hellinga, H. W. (2004) Computational design of a biologically active enzyme, *Science 304*, 1967−1971.
35. Zanghellini, A., Jiang, L., Wollacott, A. M., Cheng, G., Meiler, J., Althoff, E. A., Rothlisberger, D., and Baker, D. (2006) New algorithms and an *in silico* benchmark for computational enzyme design, *Protein Sci. 15*, 2785−2794.
36. Zhi, W., Srere, P. A., and Evans, C. T. (1991) Conformational stability of pig citrate synthase and some active-site mutants, *Biochemistry 30*, 9281−9286.
37. Meiering, E. M., Serrano, L., and Fersht, A. R. (1992) Effect of active-site residues in barnase on activity and stability, *J. Mol. Biol. 225*, 585−589.
38. Shoichet, B. K., Baase, W. A., Kuroki, R., and Matthews, B. W. (1995) A relationship between protein stability and protein function, *Proc. Natl. Acad. Sci. U.S.A. 92*, 452−456.
39. Beadle, B. M., and Shoichet, B. K. (2002) Structural bases of stability-function tradeoffs in enzymes, *J. Mol. Biol. 321*, 285−296.
40. Mukaiyama, A., Haruki, M., Ota, M., Koga, Y., Takano, K., and Kanaya, S. (2006) A hyperthermophilic protein acquires function at the cost of stability, *Biochemistry 45*, 12673−12679.
41. Kast, P., Asif-Ullah, M., and Hilvert, D. (1996) Is chorismate mutase a prototypic entropy trap? − Activation parameters for the *Bacillus subtilis* enzyme, *Tetrahedron Lett. 37*, 2691−2694.
42. Gamper, M., Hilvert, D., and Kast, P. (2000) Probing the role of the C-terminus of *Bacillus subtilis* chorismate mutase by a novel random protein-termination strategy, *Biochemistry 39*, 14087−14094.
43. Zhang, S., Wilson, D. B., and Ganem, B. (2003) An engineered chorismate mutase with allosteric regulation, *Bioorg. Med. Chem. 11*, 3109−3114.
44. Becktel, W. J., and Schellman, J. A. (1987) Protein stability curves, *Biopolymers 26*, 1859−1877.
45. Kast, P., Tewari, Y. B., Wiest, O., Hilvert, D., Houk, K. N., and Goldberg, R. N. (1997) Thermodynamics of the conversion of chorismate to prephenate: Experimental results and theoretical predictions, *J. Phys. Chem. B 101*, 10976−10982.
46. Bloom, J. D., Silberg, J. J., Wilke, C. O., Drummond, D. A., Adami, C., and Arnold, F. H. (2005) Thermodynamic prediction of protein neutrality, *Proc. Natl. Acad. Sci. U.S.A. 102*, 606−611.
47. Bershtein, S., Segal, M., Bekerman, R., Tokuriki, N., and Tawfik, D. S. (2006) Robustness-epistasis link shapes the fitness landscape of a randomly drifting protein, *Nature 444*, 929−932.
48. Bloom, J. D., Arnold, F. H., and Wilke, C. O. (2007) Breaking proteins with mutations: Threads and thresholds in evolution, *Mol. Syst. Biol. 3*, 76.
49. Shortle, D., and Lin, B. (1985) Genetic analysis of staphylococcal nuclease: Identification of three intragenic "global" supressors of nuclease-minus mutations, *Genetics 110*, 539−555.
50. Loeb, D. D., Swanstrom, R., Everitt, L., Manchester, M., Stamper, S. E., and Hutchison, C. A. (1989) Complete mutagenesis of the HIV-1 protease, *Nature 340*, 397−400.
51. Bowie, J. U., Reidhaar-Olson, J. F., Lim, W. A., and Sauer, R. T. (1990) Deciphering the message in protein sequences: Tolerance to amino acid substitutions, *Science 247*, 1306−1310.
52. Rennell, D., Bouvier, S. E., Hardy, L. W., and Poteete, A. R. (1991) Systematic mutation of bacteriophage T4 lysozyme, *J. Mol. Biol. 222*, 67−87.
53. Markiewicz, P., Kleina, L. G., Cruz, C., Ehret, S., and Miller, J. H. (1994) Genetic studies of the *lac* repressor XIV: Analysis of 4000 altered *Escherichia coli lac* repressors reveals essential and non-essential residues, as well as "spacers" which do not require a specific sequence, *J. Mol. Biol. 240*, 421−433.
54. Guo, H. H., Choe, J., and Loeb, L. A. (2004) Protein tolerance to random amino acid change, *Proc. Natl. Acad. Sci. U.S.A. 101*, 9205−9210.
55. Liu, L., and Santi, D. V. (1993) Asparagine 229 in thymidylate synthase contributes to, but is not essential for, catalysis, *Proc. Natl. Acad. Sci. U.S.A. 90*, 8604−8608.
56. Warren, M. S., Marolewski, A. E., and Benkovic, S. J. (1996) A rapid screen of active site mutants in glycinamide ribonucleotide transformylase, *Biochemistry 35*, 8855−8862.
57. Axe, D. D., Foster, N. W., and Fersht, A. R. (1998) A search for single substitutions that eliminate enzymatic function in a bacterial ribonuclease, *Biochemistry 37*, 7157−7166.
58. Aurora, R., and Rose, G. D. (1998) Helix capping, *Protein Sci. 7*, 21−38.
59. Doig, A. J., and Baldwin, R. L. (1995) N- and C-capping preferences for all 20 amino acids in α-helical peptides, *Protein Sci. 4*, 1325−1336.
60. Marshall, S. A., Morgan, C. S., and Mayo, S. L. (2002) Electrostatics significantly affect the stability of designed homeodomain variants, *J. Mol. Biol. 316*, 189−199.
61. Richardson, J. S., and Richardson, D. C. (1988) Amino acid preferences for specific locations at the ends of α-helices, *Science 240*, 1648−1652.
62. Serrano, L., and Fersht, A. R. (1989) Capping and α-helix stability, *Nature 342*, 296−299.
63. Doig, A. J., MacArthur, M. W., Stapley, B. J., and Thornton, J. M. (1997) Structures of N-termini of helices in proteins, *Protein Sci. 6*, 147−155.
64. Altschul, S. F., Madden, T. L., Schaffer, A, A., Zhang, J. H., Zhang, Z., Miller, W., and Lipman, D. J. (1997) Gapped BLAST and PSI-BLAST: A new generation of protein database search programs, *Nucleic Acids Res. 25*, 3389−3402.
65. Pruitt, K. D., Tatusova, T., and Maglott, D. R. (2005) NCBI Reference Sequence (RefSeq): a curated non-redundant sequence database of genomes, transcripts and proteins, *Nucleic Acids Res. 33*, D501−D504.
66. Taylor, S. V., Walter, K. U., Kast, P., and Hilvert, D. (2001) Searching sequence space for protein catalysts, *Proc. Natl. Acad. Sci. U.S.A. 98*, 10596−10601.
67. MacBeath, G., Kast, P., and Hilvert, D. (1998) Redesigning enzyme topology by directed evolution, *Science 279*, 1958−1961.
68. Vamvaca, K., Vögeli, B., Kast, P., Pervushin, K., and Hilvert, D. (2004) An enzymatic molten globule: Efficient coupling of folding and catalysis, *Proc. Natl. Acad. Sci. U.S.A. 101*, 12860−12864.
69. Lyne, P. D., Mulholland, A. J., and Richards, W. G. (1995) Insights into chorismate mutase catalysis from a combined QM/MM simulation of the enzyme reaction, *J. Am. Chem. Soc. 117*, 11345−11350.
70. Davidson, M. M., Gould, I. R., and Hillier, I. H. (1996) The mechanism of the catalysis of the Claisen rearrangement of chorismate to prephenate by the chorismate mutase from *Bacillus subtilis*. A molecular mechanics and hybrid quantum mechanical/molecular mechanical study, *J. Chem. Soc., Perkin Trans. 2*, 525−532.
71. Hall, R. J., Hindle, S. A., Burton, N. A., and Hillier, I. H. (2000) Aspects of hybrid QM/MM calculations: The treatment of the QM/MM interface regions and geometry optimization with an application to chorismate mutase, *J. Comp. Chem. 21*, 1433−1441.
72. Worthington, S. E., Roitberg, A. E., and Krauss, M. (2001) An MD/QM study of the chorismate mutase-catalyzed Claisen rearrangement reaction, *J. Phys. Chem. B 105*, 7087−7095.
73. Guo, H., Cui, Q., Lipscomb, W. N., and Karplus, M. (2001) Substrate conformational transitions in the active site of chorismate mutase: Their role in the catalytic mechanism, *Proc. Natl. Acad. Sci. U.S.A. 98*, 9032−9037.
74. Marti, S., Andres, J., Moliner, V., Silla, E., Tunon, I., Bertran, J., and Field, M. J. (2001) A hybrid potential reaction path and free energy study of the chorismate mutase reaction, *J. Am. Chem. Soc. 123*, 1709−1712.
75. Lee, Y. S., Worthington, S. E., Krauss, M., and Brooks, B. R. (2002) Reaction mechanism of chorismate mutase studied by the combined potentials of quantum mechanics and molecular mechanics, *J. Phys. Chem. B 106*, 12059−12065.
76. Guimarães, C. R. W., Repasky, M. P., Chandrasekhar, J., Tirado-Rives, J., and Jorgensen, W. L. (2003) Contributions of conformational compression and preferential transition state stabilization to the rate enhancement by chorismate mutase, *J. Am. Chem. Soc. 125*, 6892−6899.
77. Štrajbl, M., Shurki, A., Kato, M., and Warshel, A. (2003) Apparent NAC effect in chorismate mutase reflects electrostatic transition state stabilization, *J. Am. Chem. Soc. 125*, 10228−10237.

78. Hur, S., and Bruice, T. C. (2003) The near attack conformation approach to the study of the chorismate to prephenate reaction, *Proc. Natl. Acad. Sci. U.S.A. 100*, 12015−12020.
79. Crespo, A., Scherlis, D. A., Marti, M. A., Ordejon, P., Roitberg, A. E., and Estrin, D. A. (2003) A DFT-based QM-MM approach designed for the treatment of large molecular systems: Application to chorismate mutase, *J. Phys. Chem. B 107*, 13728−13736.
80. Guo, H., Cui, Q., Lipscomb, W. N., and Karplus, M. (2003) Understanding the role of active-site residues in chorismate mutase catalysis from molecular-dynamics simulations, *Angew. Chem., Int. Ed. 42*, 1508−1511.
81. Ranaghan, K. E., and Mulholland, A. J. (2004) Conformational effects in enzyme catalysis: QM/MM free energy calculations of the 'NAC' contribution in chorismate mutase, *Chem. Commun*. 1238−1239.
82. Ranaghan, K. E., Ridder, L., Szefczyk, B., Sokalski, W. A., Hermann, J. C., and Mulholland, A. J. (2004) Transition state stabilization and substrate strain in enzyme catalysis: *ab initio* QM/MM modeling of the chorismate mutase reaction, *Org. Biomol. Chem. 2*, 968−980.
83. Szefczyk, B., Mulholland, A. J., Ranaghan, K. E., and Sokalski, W. A. (2004) Differential transition-state stabilization in enzyme catalysis: Quantum chemical analysis of interactions in the chorismate mutase reaction and prediction of the optimal catalytic field, *J. Am. Chem. Soc. 126*, 16148−16159.
84. Guimarães, C. R. W., Udier-Blagovic, M., Tubert-Brohman, I., and Jorgensen, W. L. (2005) Effects of Arg90 neutralization on the enzyme-catalyzed rearrangement of chorismate to prephenate, *J. Chem. Theory Comput. 1*, 617−625.
85. Claeyssens, F., Ranaghan, K. E., Manby, F. R., Harvey, J. N., and Mulholland, A. J. (2005) Multiple high-level QM/MM reaction paths demonstrate transition-state stabilization in chorismate mutase: Correlation of barrier height with transition-state stabilization, *Chem. Commun.* 5068−5070.
86. Crespo, A., Marti, M. A., Estrin, D. A., and Roitberg, A. E. (2005) Multiple-steering QM-MM calculation of the free energy profile in chorismate mutase, *J. Am. Chem. Soc. 127*, 6940−6941.
87. Ishida, T., Fedorov, D. G., and Kitaura, K. (2006) All electron quantum chemical calculation of the entire enzyme system confirms a collective catalytic device in the chorismate mutase reaction, *J. Phys. Chem B 110*, 1457−1463.
88. Hur, S., and Bruice, T. C. (2002) The mechanism of catalysis of the chorismate to prephenate reaction by the *Escherichia coli* mutase enzyme, *Proc. Natl. Acad. Sci. U.S.A. 99*, 1176−1181.
89. Hur, S., and Bruice, T. C. (2003) Comparison of formation of reactive conformers (NACs) for the Claisen rearrangment of chorismate to prephenate in water and in the *E. coli* mutase: The efficiency of the enzyme catalysis, *J. Am. Chem. Soc. 125*, 5964−5972.
90. Zhang, X. D., Zhang, X. H., and Bruice, T. C. (2005) A definitive mechanism for chorismate mutase, *Biochemistry 44*, 10443−10448.
91. Khanjin, N. A., Snyder, J. P., and Menger, F. M. (1999) Mechanism of chorismate mutase: Contribution of conformational restriction to catalysis in the Claisen rearrangement, *J. Am. Chem. Soc. 121*, 11831−11846.
92. Bone, R., Silen, J. L., and Agard, D. A. (1989) Structural plasticity broadens the specificity of an engineered protease, *Nature 339*, 191−195.
93. Gerlt, J. A., Babbitt, P. C., and Rayment, I. (2005) Divergent evolution in the enolase superfamily: The interplay of mechanism and specificity, *Arch. Biochem. Biophys. 433*, 59−70.
94. Aharoni, A., Gaidukov, L., Kheronsky, O., Gould, S. M., Roodveldt, C., and Tawfik, D. S. (2005) The 'evolvability' of promiscuous protein functions, *Nat. Genet. 37*, 73−76.
95. Yoshikuni, Y., Ferrin, T. E., and Keasling, J. D. (2006) Designed divergent evolution of enzyme function, *Nature 440*, 1078−1082.

BI700215X